

H_3^+ Spectroscopy and the Ionization Rate of Molecular Hydrogen in the Central Few Parsecs of the Galaxy [†]

Miwa Goto,^{*,‡} Nick Indriolo,[¶] T. R. Geballe,[§] and T. Usuda^{||}

Universitäts-Sternwarte München, Scheinerstr. 1, D-81679 Munich, Germany, Department of Physics and Astronomy, 3400 N. Charles St., Baltimore, MD 21218, USA, 670 North A‘ohoku Place, Hilo, HI 96720, USA, and 650 North A‘ohoku Place, Hilo, HI 96720, USA

E-mail: mgoto@usm.lmu.de

Abstract

We report observations and analysis of infrared spectra of H_3^+ and CO lines in the Galactic center, within a few parsecs of the central black hole, Sgr A*. We find a cosmic ray ionization rate typically an order of magnitude higher than outside the Galactic center. Notwithstanding, the elevated cosmic ray ionization rate is 4 orders of magnitude too short to match the proton energy spectrum as inferred from the recent discovery of the TeV γ -ray source in the vicinity of Sgr A*.

Introduction

H_3^+ and the cosmic ray ionization rate

The ionization of molecular hydrogen by cosmic rays – mainly high energy protons, helium nuclei, and electrons – has diverse and important

influences on the physics and chemistry of interstellar molecular clouds. It is a significant heat source in interstellar clouds, through the secondary electrons liberated in the ionization process. If a cloud is even slightly ionized, its internal motions are restricted by the ambient magnetic field. In star forming clouds the timescale for cloud collapse is affected by the ionization fraction. Ion-neutral reactions, which generally proceed with large Langevin rates, are the main propellant of interstellar chemistry; neutral-neutral reactions have reaction barriers and are consequently prohibitively slow at the low-temperatures of interstellar molecular clouds. Thus chemistry in molecular clouds is driven by the cosmic ray ionization of H_2 .

Interstellar molecular clouds come in a range of sizes and densities, but for many purposes may be regarded as consisting of two types: diffuse clouds ($10 \text{ cm}^{-3} < n < 3 \times 10^2 \text{ cm}^{-3}$) and dense clouds ($n > 3 \times 10^2 \text{ cm}^{-3}$). Regardless of the cloud type the ionization of H_2 within a cloud occurs almost exclusively by cosmic rays collisions. Photons capable of ionizing H_2 (i.e., with $E > 15.4 \text{ eV}$)¹ are consumed outside the cloud or on its surface by the ionization of atomic hydrogen (ionization potential 13.6 eV) and/or absorption by dust particles and thus have little or no effect on physics and chemistry in the interior. Ultraviolet photons with less than this energy penetrate diffuse clouds; as a result hydrogen in them is only partly in molecular

[†]Based on data collected in the course of CRIRES Science Verification program (60.7A-9057) and open-use program (079.C-0874) at the VLT on Cerro Paranal (Chile), which is operated by the European Southern Observatory (ESO). Based also on data collected at Subaru Telescope, which is operated by the National Astronomical Observatory of Japan.

*To whom correspondence should be addressed

[‡]Universitäts-Sternwarte München

[¶]Johns Hopkins University

[§]Gemini Observatory

^{||}Subaru Telescope

form and the abundant element carbon is mainly atomic and singly ionized due to its low ionization potential (11.3 eV). In dense clouds dust does not allow near-ultraviolet radiation to penetrate. As a result dense clouds are essentially fully molecular (e.g., virtually all H in H₂ and all C in CO).

The ionization collisional cross-section of H₂ peaks at 70 keV^{2,3} and decreases to higher energy as a power law. It is thought that the cosmic rays that contribute most significantly to the ionization of H₂ within clouds have energies, $E < 100$ MeV. Their intrinsic spectrum, however, cannot be directly measured from inside the solar system, because the influx of cosmic rays with $E < 1$ GeV is deflected by the solar wind and magnetic field. One must therefore rely on indirect techniques to determine the cosmic ray ionization rate of molecular hydrogen, ζ_2 , either by appealing to the energetics of the interstellar medium,⁴ or to the chemistry by observing the abundances of molecules formed in reactions triggered by cosmic ray ionization of H₂, such as OH, HD, HCO⁺,⁵⁻⁷ or H₃⁺.

Of these molecules H₃⁺, first detected in molecular clouds 17 years ago,⁸ is the most reliable probe of the cosmic ray ionization rate of molecular hydrogen, simply because the number of the reactions involved in its production is effectively the minimum, one. In a molecular cloud, once H₂ is ionized, the reaction, $\text{H}_2^+ + \text{H}_2 \rightarrow \text{H}_3^+ + \text{H}$, is so rapid compared to the other competing processes that virtually all H₂⁺ produced by cosmic rays quickly is converted into H₃⁺. The H₃⁺ formation rate is therefore directly proportional to the cosmic ray ionization rate ζ_2 . Destruction of H₃⁺ is dominated by fast electron dissociative recombination in diffuse clouds and by chemical reaction with CO to form HCO⁺ in dense clouds. Both reactions have been well studied in the laboratory. Equating creation and destruction rates one obtains (1)

$$n(\text{H}_2) \zeta_2 = k_{\text{CO}} n(\text{H}_3^+) n(\text{CO})$$

in dense clouds and (2)

$$n(\text{H}_2) \zeta_2 = k_e n(\text{H}_3^+) n(e)$$

in diffuse clouds, where k_e and k_{CO} are the dominant H₃⁺ destruction rate coefficients for the two

types of clouds, and k_e is larger than k_{CO} by roughly two orders of magnitude at typical cloud temperatures. In each type of cloud, however, the steady state density of H₃⁺ depends linearly on the cosmic ray ionization rate.

High local cosmic ray ionization rate

Until a decade ago, ζ_2 was simplistically considered to be roughly uniform throughout much of the Galaxy, with values within a factor of 3 of $3 \times 10^{-17} \text{ s}^{-1}$, because the great penetrating power of typical cosmic rays was thought to smooth out local influences of particle accelerators. Studies of interstellar clouds using H₃⁺ have now conclusively demonstrated that this is not the case. They have revealed that values of ζ_2 in diffuse clouds are on average an order of magnitude higher than in dense molecular clouds,⁹⁻¹¹ a finding most easily explained by a large and heretofore unrecognized population of low energy (< 10 MeV) cosmic rays, which penetrate diffuse clouds much more effectively than dense clouds.¹² In addition, real and large differences in the rates deduced for different diffuse clouds have been found.¹⁰ Finally, a direct connection between a particle acceleration source and the local cosmic ray ionization rate has been demonstrated by Indriolo et al.¹³ near the supernova remnant IC 443, where $\zeta_2 = 2 \times 10^{-15} \text{ s}^{-1}$, an order of magnitude higher than in typical diffuse clouds in the Galaxy.

Much higher ionization rates than those reported above are predicted in especially energetic environments, within galactic nuclei or near the highest energy supernovae. Yusef-Zadeh et al.¹⁴ has argued that the ionization rate could be as high as $5 \times 10^{-13} \text{ s}^{-1}$ near the center of the Milky Way galaxy, in locations where high energy electrons that produce X-ray and non-thermal radio emission encounter dense molecular clouds. Likewise, Tatischeff et al.¹⁵ estimate that the ionization rate in the Galactic center's Arches Cluster is $1 \times 10^{-13} \text{ s}^{-1}$. The prediction by Becker et al.¹⁶ (also Black¹⁷) is even more extreme: ionization rates of $\sim 1 \times 10^{-12} \text{ s}^{-1}$ near γ -ray emitting supernova remnants, if they are the principal sources of Galactic cosmic rays.

The subject of this paper is the ionization rate in what may be the closest dense molecular cloud

to the Galactic center where $\text{H}_3^+ R(2,2)^l$ absorption was first detected in the interstellar medium by Goto et al. (2008).¹⁸ The ionization rate measured using the new data with improved velocity resolution is compared to the ionization rates expected from the X-ray and the cosmic ray flux in the central few parsecs of the Galactic center.

The Central Molecular Zone

As suggested above, the very innermost region of the Galaxy is a site where one might expect to find extreme values of ζ_2 . The rate per unit volume of supernova outbursts in the center is estimated to be 0.04 times per century,¹⁹ 2000 times higher than the Milky Way average.^{20,21} Despite these and other violent events and the generally high energy density, molecular gas is abundant in the center. Indeed the central 200 pc of the Galaxy, known as the Central Molecular Zone,²² contains one tenth of the entire molecular mass of the Milky Way in its scant 0.001% of the volume.²²

A significant fraction of the molecular gas in the Central Molecular Zone is found in giant and dense molecular clouds, which take up only a small fraction of the volume of the Central Molecular Zone. However, spectroscopy of H_3^+ has recently shown that molecules also are plentiful outside of those clouds. Indeed a large fraction of the volume of the Central Molecular Zone is filled with warm (~ 250 K) and much more rarified ($\leq 100 \text{ cm}^{-3}$) molecular gas.^{23,24} Within this diffuse molecular gas ζ_2 has been estimated to be $(2-7) \times 10^{-15} \text{ s}^{-1}$,²⁴ roughly an order of magnitude higher than the average value for diffuse clouds outside of the center.

The central few parsecs

Here we focus on molecular gas within the central few parsecs of the Central Molecular Zone, a tiny region containing a massive black hole Sgr A*,²⁵ a multitude of old stars, and a "Central Cluster" of $\sim 10^2$ young, hot and massive stars (also known as the nuclear star cluster²⁶). A sketch of this "laboratory" is shown in 1. The principal gaseous structure there is the Circumnuclear Disk,^{27,28} a clumpy stream of molecular clouds, with inner radius 1.5 pc, orbiting Sgr A*. The gas density drops

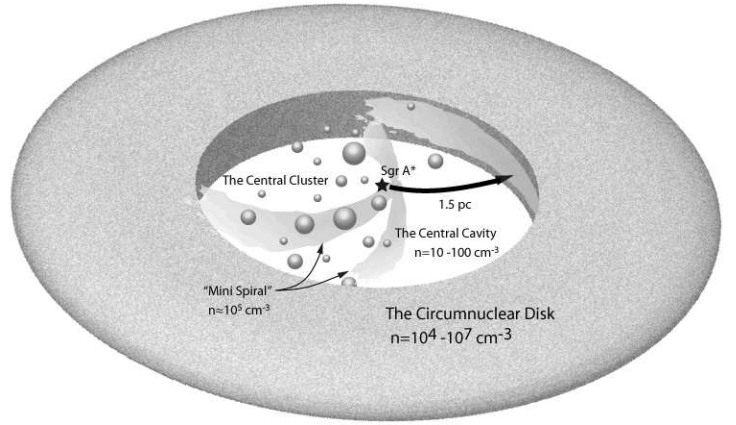


Figure 1: Schematic view of the central few parsecs of the Galaxy, showing the central black hole (Sgr A*), members of the Central Cluster of massive stars, the Circumnuclear disk, and molecular gas within the Central Cavity.

from $10^4-10^7 \text{ cm}^{-3}$ within the Disk^{29,30} to $10-100 \text{ cm}^{-3}$ in the Central Cavity,³¹ the low-density region between Sgr A* and the inner surface of the Circumnuclear Disk. Gas in the Central Cavity is partly ionized by the radiation from the stars in the Central Cluster.^{32,33} The high-mass stars in the Central Cluster formed approximately 6 Myrs ago, and are now at the end of the main-sequence evolutionary phase.³⁴ Among them, two of the brightest at mid-infrared wavelengths are GCIRS 1W and GCIRS 3. Gas in the cavity is partly ionized by the hot stars in the Central Cluster. The radiation and the stellar winds from those stars are the main source of radiation and kinetic energy injected into the Central Cavity.^{35,36} The HII region of the Central Cavity together with a few distinct streamers of the molecular clouds ("Mini-spiral") are collectively called Sgr A West.^{37,38}

Observations

Absorption spectroscopy in astronomy is similar to absorption spectroscopy in the laboratory. In each case the experimental setup consists of a background light source, the spectrograph, and a sample placed between the two. For this study the light sources were GCIRS 3 and GCIRS 1W in the Central Cluster within a few tenths of a parsec of Sgr A* as viewed in the plane of the sky. The spec-

trograph was the Cryogenic Infrared Echelle Spectrograph (CRIRES)³⁹ ($\lambda/\Delta\lambda = 50,000\text{--}100,000$) on the Very Large Telescope (VLT) at the Paranal Observatory in Chile. The sample was the gas between the Earth and the Galactic center, which are separated by 8 kpc.^{40,41} In actuality almost all of the intervening gas is within the Central Molecular Zone or associated with Galactic spiral arms between the Central Molecular Zone and the Earth.

The targeted spectral lines of H_3^+ were v_2 vibrational transitions from the $(J,K)=(1,1)$, $(3,3)$ and $(2,2)$ levels at $\lambda = 3.5\text{--}3.7 \mu\text{m}$. Each of these lines is an important diagnostic. The line from the $(1,1)$ level provides in a straightforward manner the column density in the lowest energy level. The $(3,3)$ level, 361 K above $(1,1)$ is metastable; when collisionally populated, as is the case in the Central Molecular Zone, it serves as a (density-independent) thermometer. The $(2,2)$ level, at an intermediate energy, has a lifetime against spontaneous emission of 27 days; for temperatures not much lower than its excitation, 150 K, lines from $(2,2)$ are densitometers for low density clouds. In addition to these lines of H_3^+ , the fundamental band of ^{13}CO at $4.7 \mu\text{m}$ was observed, in part to help distinguish between gas in the Central Molecular Zone and the foreground arms. (Lines of ^{12}CO are also present but are too strong to be useful in this regard.)

The data were obtained on several nights in 2006–2008. Standard data reduction techniques were employed (e.g. Goto et al. 2008¹⁸). The final spectra, shown in Figs. 2–4, are corrected for instrumental transmission and atmospheric absorption and have been wavelength-calibrated to an accuracy corresponding to $\pm 1 \text{ km s}^{-1}$.

Results

Gas in the Central Molecular Zone

Spectra toward GCIRS 3 and GCIRS 1W of the three H_3^+ lines and the low-lying $^{13}\text{CO } P(1)$ line are compared in 2. Spectra of a much wider range of ^{13}CO lines toward GCIRS 3 are shown in 3. As can be seen in 2, with the exception of the density-sensitive $\text{H}_3^+ R(2,2)^l$ line, each line shows absorption over a wide velocity range. From the forego-

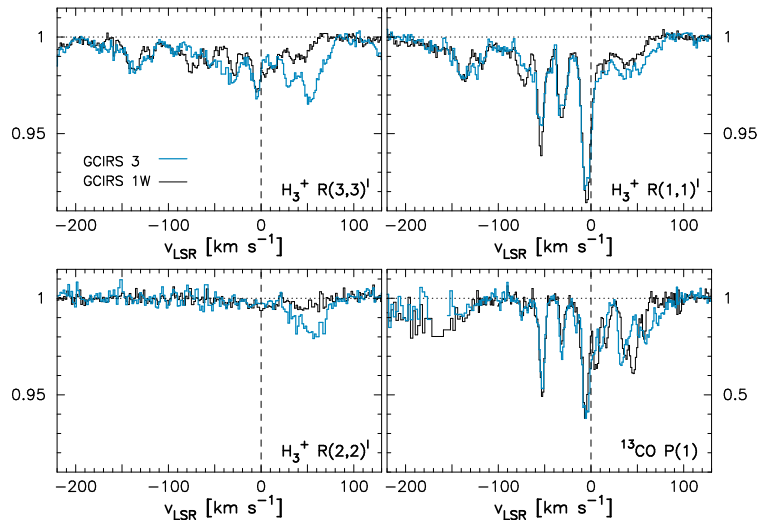


Figure 2: H_3^+ and $^{13}\text{CO } v=1-0 P(1)$ spectra toward GCIRS 3 (blue) and GCIRS 1W (black).

ing discussion the presence of the $R(3,3)^l$ line and absence of the $R(2,2)^l$ line over much of this range implies that at most velocities where warm molecular gas exists it is at low density.

For the most part the pairs of spectra of the other three lines have nearly identical profiles over much of their velocity ranges. This is not surprising, as both the Central Molecular Zone and the intervening Galactic arms are enormous structures compared to the separation of the GCIRS 3 and GCIRS 1W lines of sight, $\sim 0.3 \text{ pc}$ (one lightyear). The physical conditions in the adjacent absorbing columns would not be expected to differ much over such a small separation distance. On the other hand, the Circumnuclear disk and gas physically associated with it are much smaller so it would not be surprising to see differences in that part of the absorption profile contributed by them.

Previous studies of H_3^+ and CO lines toward these and other infrared sources in the Galactic center over much wider range of sightlines than those shown here, together with knowledge of Galactic structure gleaned mainly from radio observations, allow one to clearly associate large portions of these line profiles with gas in the Central Molecular Zone and the foreground arms.^{18,24,42} The narrow absorption features near 0, -30 and -50 km s^{-1} , common to the $\text{H}_3^+ R(1,1)^l$ and ^{13}CO lines are associated with cold and dense molecular gas in the foreground Galactic arms. On the other hand, the shallow trough of absorption seen

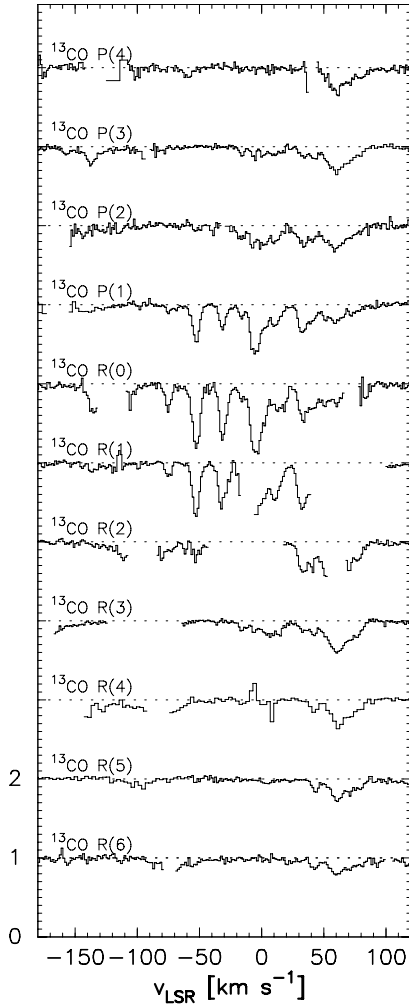


Figure 3: Spectra of individual ^{13}CO $v=1-0$ lines toward GCIRS 3. Gaps in the individual profiles correspond to wavelengths intervals of poor atmospheric transmission and/or to wavelengths where ^{12}CO $v=1-0$ lines overlap.

in the $R(1,1)^l$ line profile to extend roughly from -200 to 0 km s^{-1} , nearly perfectly matched by the full $R(3,3)^l$ profile, but conspicuously absent in the both $R(2,2)^l$ and ^{13}CO profiles, must be produced by warm and low-density gas which, while containing H_2 (otherwise there would be no H_3^+), contains little or no CO . This description is the calling card of diffuse molecular gas, as introduced earlier in this paper. The wide spatial and velocity extents of these absorptions and the warm temperature of the gas require that the gas be located within the Central Molecular Zone, and expanding outward from the center.

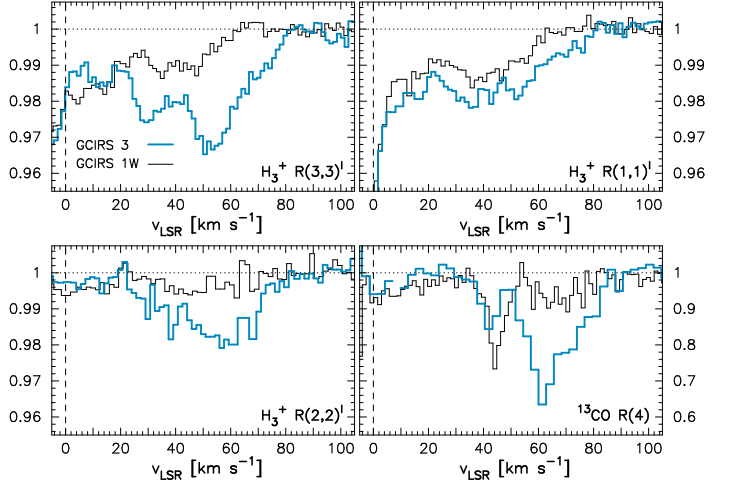


Figure 4: An expanded view of 2 at the positive velocity $0-100$ km s^{-1} . The velocity profile of the ^{13}CO $1-0$ $R(4)$ line is shown, in place of the $P(1)$ line.

Gas in the Central Cavity

The largest differences between the line profiles toward GCIRS 1W and GCIRS 3 in 2 are at velocities greater than about $+20$ km s^{-1} . This velocity range is shown in more detail in 4; note that in this figure we show the ^{13}CO $R(4)$ line as it is more representative of the ^{13}CO line profiles in this velocity range than the $P(1)$ line shown in 2.

In general the sightline toward GCIRS 3 produces stronger absorptions than GCIRS 1W at $v > +20$ km s^{-1} , but there also are differences in the shapes of the profiles between the two objects. Toward GCIRS 3 the absorption maxima of all the three H_3^+ lines occur at $\sim +50$ km s^{-1} . Absorption by all but the lowest lying ^{13}CO lines also peak near that velocity (see 3 and the bottom right panel of 4).

Apart from GCIRS 1W and GCIRS 3 none of the observed sightlines through the Central Molecular Zone within 30 pc of the center produce absorption at $v > +20$ km s^{-1} in any of the H_3^+ lines.¹⁸ Moreover, the presence of both the excited H_3^+ lines and the ^{13}CO absorption from excited rotational levels (see 3) implies that the absorbing gas is warm. Such absorptions cannot be produced by the cold gas of the foreground spiral arms, but instead must arise in the Galactic center.

Despite the similarity in velocities we conclude that these absorptions by H_3^+ and CO do not arise

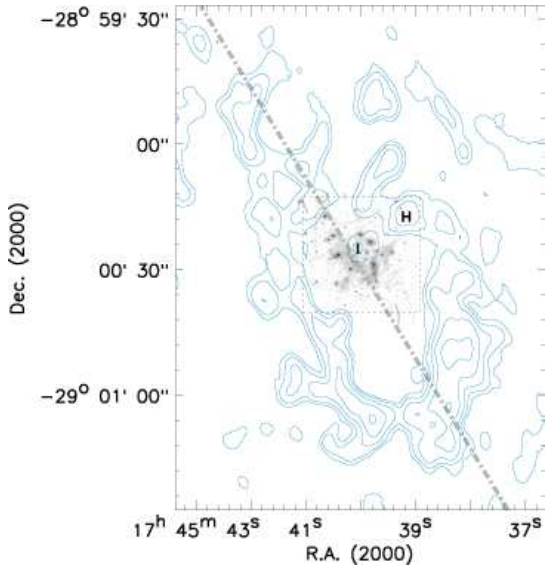


Figure 5: HCN $J=4-3$ map of the Circumnuclear Disk²⁸ (blue contours) overlaid with a VLT K -band image of the Central Cluster. The lowest contour level is $1.6 \text{ J m beam}^{-1} \text{ s}^{-1}$ (2σ). The dot-dash line denotes constant latitude and is parallel to the Galactic plane. Clumps H and I, as identified by Montero-Castaño et al., are labeled.

in the well-known “+50 km s^{-1} ” giant molecular cloud (M-0.02-0.07),^{43,44} which is located within the Central Molecular Zone, has dimensions of roughly 20–30 pc, and is known from a multitude of radio wavelength studies to extend across the sightlines to GCIRS 1W and GCIRS 3. The large differences between the absorption profiles at positive velocities in GCIRS 3 and GCIRS 1W tends to rule out the absorption occurring in such a large cloud.

This foregoing suggests that the absorption at positive velocities occurs very close to GCIRS 3 and we thus consider the possibility that the absorption arises in the Circumnuclear disk and/or dense clouds that come off from the Circumnuclear disk to the Central Cavity. 5 is a contour map of the Circumnuclear disk in the HCN $J=4-3$ line obtained by Montero-Castaño et al.,²⁸ on which is superimposed a K -band ($\lambda = 2.2 \mu\text{m}$) image of the stars in the Central Cluster retrieved from the VLT archive. As is shown in an expanded view (6) a compact “clump I” (Montero-Castaño et al.), which may be physically connected to the Circumnuclear disk, positionally coincides with GCIRS 3,

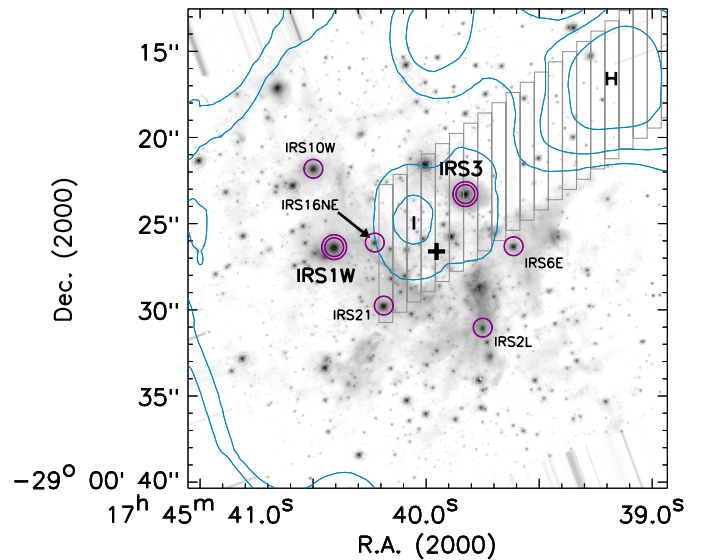


Figure 6: Expanded view of the central part of 5. The cross is the position of Sgr A*. The positions of the apertures where the spectra in 7 were extracted are marked with gray rectangles.

while the line of sight to GCIRS 1W is clear. Note that, as $n_{\text{crit}} \sim 10^8 \text{ cm}^{-3}$ for the HCN $J=4-3$ shown in 5, this transition predominantly traces the highest density portions of the disk. Lower density molecular gas with much weaker HCN emission in this line could extend considerably inward from the outermost contours.

To investigate the relationship between clump I and the Circumnuclear disk, HCN line emission spectra were extracted along a line connecting the densest portion of the Circumnuclear disk at clump H²⁸ with clump I and are shown in 7. From them it is clear that (1) the Circumnuclear disk gas at clump H, seen at LSR velocities of +50–+60 km s^{-1} , extends inward across the sightline to GCIRS 3 and close to clump I, but not to GCIRS 1W, and (2) clump I itself is mainly associated with gas at a radial velocity of $\sim -30 \text{ km s}^{-1}$. It would then appear that -30 km s^{-1} gas in clump I is not physically connected to the Disk. As can be seen in 8 at GCIRS 3 the HCN emission line profile near +50 km s^{-1} is an excellent match to the $\text{H}_3^+ R(2,2)^l$ absorption line, not only in its line center, but also in its line shape. We interpret this as strong evidence that the absorption toward GCIRS 3 centered at +50 km s^{-1} arises largely in this arm of molecular gas extending inward to the

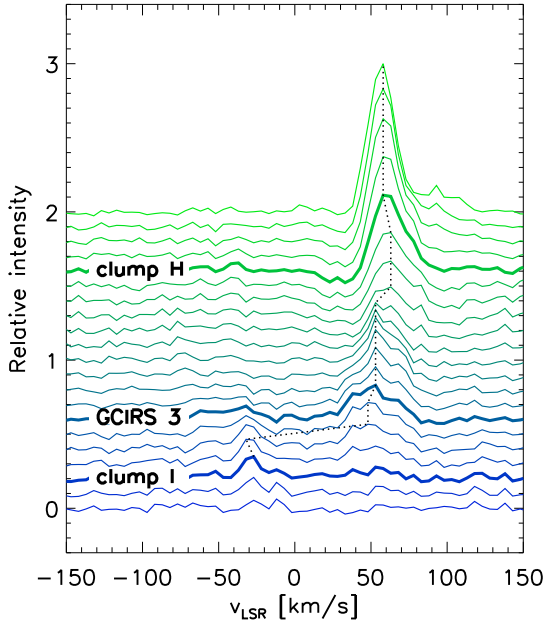


Figure 7: HCN $J=4-3$ emission line spectra extracted from the apertures shown in 6 from clump H through the position of GCIRS 3 to clump I. Velocities of maximum emission are connected by a dotted line.

west of clump I from the Circumnuclear disk.

Temperature and density

We convert the measured equivalent widths of the H_3^+ absorption lines in the interval $+20$ to $+80 \text{ km s}^{-1}$ to column densities in the (1,1), (2,2) and (3,3) states using standard procedures (see Goto et al. 2008) and utilizing the dipole transition moments given by Neale et al..⁴⁵ The absorptions arising in the diffuse clouds at the same velocity range, whose presence is apparent in the spectra of GCIRS 1W, were removed by subtracting the spectra of GCIRS 1W from those of GCIRS 3 prior to the measurement of the equivalent widths. Using the steady state analysis of Oka and Epp⁴⁶ one can then use the relative level populations to estimate the temperature and the density in the absorbing gas. We find $250 \text{ K} < T < 350 \text{ K}$ and $> 500 \text{ cm}^{-3}$ (9). This is sufficiently dense for the gas to be classified as a dense cloud. Unsurprisingly it is much warmer than the typical Galactic equivalent. The derived density is far less than the critical density of the HCN $J=4-3$ transition, suggesting that observed H_3^+ inhabits a different por-

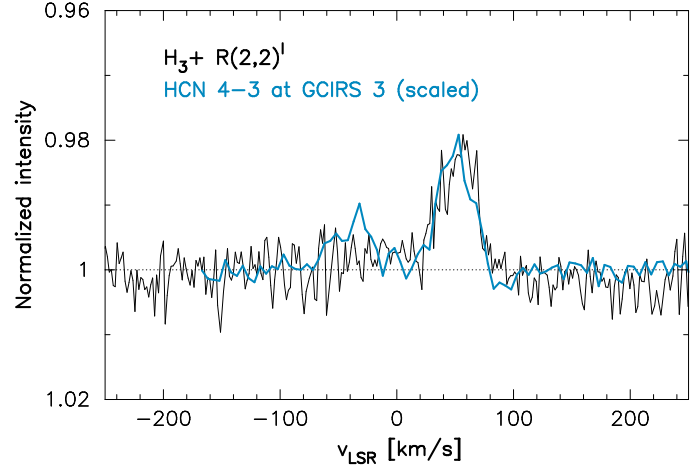


Figure 8: Comparison of the line profiles of $\text{H}_3^+ R(2,2)^l$ and HCN $J=4-3$ at the location of GCIRS 3. The HCN $J=4-3$ emission spectrum has been inverted and scaled to match the intensity of the $R(2,2)^l$ line.

tion of the cloud than the observed HCN, perhaps the outer layers. Detailed analysis of the ^{13}CO absorption feature centered at 60 km s^{-1} is complicated, as the individual transitions have widely different critical densities. However, the relative line strengths indicate temperatures exceeding 100 K and densities of $\sim 10^6 \text{ cm}^{-3}$ (see Kramer et al.⁴⁷ 2004).

The cosmic ray ionization rate

Here we derive the cosmic ray ionization rate in the $+50 \text{ km s}^{-1}$ gas on the line of sight to GCIRS 3. In Goto et al. 2008 ζ_2 was calculated assuming the cloud at $+50 \text{ km s}^{-1}$ is diffuse, as in the case for the other clouds filling the large part of the Galactic center. The gas likely has the properties of a dense cloud (i.e, it is fully molecular), as is discussed above, and therefore we use equation (1), which can be re-expressed as

$$\zeta_2 L = 2k'_L N(\text{H}_3^+) \frac{n_C}{n_H} R_x,$$

where L is the pathlength through the cloud, $N(\text{H}_3^+)$ is the observed column density of H_3^+ , $k'_L = 3 \times 10^{-9} \text{ cm}^3 \text{ s}^{-1}$ is the Langevin rate constant for the reaction $\text{H}_3^+ + \text{CO} \rightarrow \text{H}_2 + \text{HCO}^+$ taken from Anicich and Huntress⁴⁸ and Klippenstein et al.,⁴⁹ and multiplied by 1.5 to take into account the

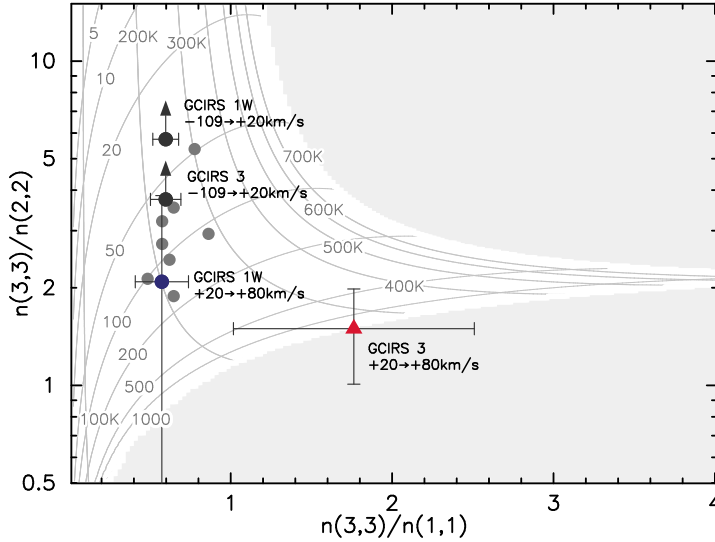


Figure 9: Comparison of the relative level populations of H_3^+ , $n(3,3)/n(2,2)$ and $n(3,3)/n(1,1)$ in the lines of sight to GCIRS 3 and GCIRS 1W, derived from the steady state analysis by Oka and Epp.⁴⁶ The gray dots correspond to other sightlines to sources in the Galactic center within 30 pc of Sgr A*¹⁸ that mostly sample the gas in the Central Molecular Zone. Note the higher temperatures and density in the gas in front of GCIRS 3 at radial velocities +20 to +80 km s^{-1} (red triangle).

other minor destruction paths (especially $\text{H}_3^+ + \text{O} \rightarrow \text{H}_2 + \text{OH}^+$ or $\rightarrow \text{H} + \text{H}_2\text{O}^+$), $\frac{n_{\text{C}}}{n_{\text{H}}}|_{\text{SV}} (= 1.6 \times 10^{-4})$ ^{50,51} is the fractional abundance of carbon relative to hydrogen in the solar vicinity, and R_x is the correction factor to take into account the higher abundances of elements other than H in the Galactic center.

We take L to be 0.1 pc, roughly half the distance between GCIRS 3, which lies behind the arm, and GCIRS 1W, where the cloud is absent, and $R_x = 3$, a conservatively low value in the range proposed to date.^{52–56} The total column density of H_3^+ is calculated by adding the column density of $N(1,1)$, $N(2,2)$, and $N(3,3)$, in addition to $N(1,0)$ published in Goto et al. (2008).¹⁸ [$N(\text{H}_3^+) = 6 \times 10^{14} \text{ cm}^{-2}$]. We thus obtain $\zeta_2 = 1.2 \times 10^{-15} \text{ s}^{-1}$.

We regard the above value for ζ_2 as a lower limit, because we have used a low value for R_x and also have assumed that the +50 km s^{-1} gas is fully molecular, which may well be the case for the dense core which produces the HCN $J=4-3$ line emission, but may not be in the outer more exposed, lower density regions where the bulk of

the H_3^+ absorption is likely to occur. The value of the ionization rate thus may not differ greatly from values of $(2-7) \times 10^{-15} \text{ s}^{-1}$ derived for the Central Molecular Zone as a whole by Oka et al. (2005).

Sources of H_2 Ionization

These values of the ionization rate are among the highest measured in the Galaxy. It is therefore of interest to consider possible sources of the ionizing particles. The black hole in Sgr A*, nearby supernova remnants, and energetic winds from stars in the Central Cluster are all potential particle accelerators. We have assumed so far that cosmic ray is the sole source of ionization of H_2 . This is probably the case for the Central Molecular Zone, where the size of the medium (~ 200 pc) is much larger than the range of the X-ray photons ($\sigma_x \approx 10^{-22} \text{ cm}^{-2}$ at 1 keV⁵⁷), therefore X-ray does not directly contribute to the ionization in much of the region, but need not be the case in the central few parsecs. There the ionization can be due to the local sources. We discuss below the H_2 ionization by the cosmic rays as well as by X-rays, and estimate the expected ζ_2 for each mechanism.

Cosmic ray ionization

The rate at which a single molecular hydrogen is ionized by an energetic proton is given by the product of the proton specific intensity, $J_p(E)$ and the ionization cross section of H_2 , $\sigma_p(E)$, integrated over energy and solid angle,

$$\zeta_2 = 4\pi \int_{E_1}^{E_2} J_p(E) \cdot \sigma_p(E) dE.$$

Ionization by the electron impact is neglected, since the energy loss through radiative processes as a result of the interaction with the interstellar magnetic field, ambient photons and charged particles is much faster, and since the ionization cross section is an order of magnitude smaller than for protons.

What kind of proton spectrum one should assume in the central few parsecs of the Galaxy? A clue comes from a high energy (up to ~ 10 TeV) γ -ray observation. A point-like TeV γ -ray source

was recently discovered in the Galactic center by the High Energy Stereoscopic System (HESS Collaboration)⁵⁸ which observes optical Cherenkov light of an electron-positron pair generated by the incidence of high energy γ -rays on the Earth's atmosphere. The source, HESS J1745–290, was subsequently localized to within a few arcminutes of Sgr A*. Aharonian and Neronov⁵⁹ argue that the most likely mechanism to produce such high energy γ -rays is neutral pion decay, precipitated by the acceleration of protons near the black hole. When such protons encounter cold nuclei in the ambient medium, proton-proton scattering produces neutral pions which subsequently decays pairs of high energy γ -ray photons. From the observed γ -ray spectrum, the energy spectrum of protons injected to the cold medium can be determined. Chernyakova et al.⁶⁰ calculated that the proton flux required to reproduce the observed γ -ray spectrum of HESS J1745–290 from 0.1 GeV to 100 TeV is $E^2 F = 1.4 \times 10^3 \text{ erg cm}^{-2} \text{ s}^{-1}$ at 1 GeV in their representation, or $7 \times 10^4 \text{ particles cm}^{-2} \text{ s}^{-1} \text{ str}^{-1} (\text{GeV/Nucleon})^{-1}$. For comparison, the standard proton flux in the Milky Way is $0.2 \text{ particles cm}^{-2} \text{ s}^{-1} \text{ str}^{-1} (\text{GeV/Nucleon})^{-1}$ at 1 GeV,^{4,12} which is 3×10^5 times smaller.

The collisional ionization of H_2 occurs via proton impact ($\text{H}_2 + \text{p} \rightarrow \text{H}_2^+ + \text{p} + \text{e}$) and electron capture ($\text{H}_2 + \text{p} \rightarrow \text{H}_2^+ + \text{H}$) and is well understood, theoretically⁶¹ and experimentally.² The combined ionization cross-section is reproduced from Rudd et al., Padovani et al.^{2,3} in 10. As $\sigma_p(E)$ is well understood, the cosmic ray ionization rate is virtually only dependent on the proton spectrum $J_p(E)$. If $J_p(E)$ is scaled up by 3×10^5 times from the Galactic standard, ζ_2 becomes larger by the same factor. Such a large ζ_2 has never been observed, not even in the Galactic center; the values that we and others have reported are only larger by factors of 10-100 than those outside the center.

There could be at least two possible explanations for this huge discrepancy: uncertain extrapolation of $J_p(E)$ to the lower energy, and the non-linear dependency of H_3^+ abundance on ζ_2 for very high values of ζ_2 .

As mentioned earlier the cosmic ray spectrum cannot be directly observed in the energy range where ionization of H_2 is most efficient (1–

10 MeV), because of the solar modulation. At much higher energies where direct observations are possible, the number flux of cosmic ray protons increases as energy decreases from TeV to GeV according to a power law, $J(E) \propto E^\alpha$, with α between -2 and -3 . At lower energies the best measurements are by the Voyagers and Pioneer spacecrafts in the outer solar system.^{62,63} Although the observations are still affected by the solar modulation, the local interstellar cosmic ray spectrum can be predicted using the latest solar modulation models.^{63–65} The intrinsic cosmic ray spectra are roughly flat at 0.1–1 GeV,⁶⁶ as is expected from the shorter range of the low energy cosmic rays ($2.5 \times 10^{20} \text{ cm}^{-2}$ for 1 MeV cosmic ray proton⁶⁷).

On the other hand, Indriolo et al.¹² found that a low-energy turnover at 0.1–1 GeV is inconsistent with the mean ionization rate inferred from H_3^+ spectroscopy. Instead the proton spectrum must continue to increase down to 1 MeV, otherwise the H_2 ionization rate is too low compared to the observed $\zeta_2 = 4 \times 10^{-16} \text{ s}^{-1}$ in diffuse clouds, an average value secured by H_3^+ spectroscopy toward more than a dozen of sightlines.¹¹ A similar conclusion is reached by Neronov et al.,⁶⁸ who analyzed γ -ray spectra of the molecular clouds close to the solar system known as the Gould Belt clouds. The observed γ -ray spectra were best reproduced by the cosmic-ray protons having power-law spectrum with a weak break (a change of the spectral index) at 9 GeV, but no turnover (change of sign of the spectral index).

The uncertain extrapolation of the cosmic ray spectrum from the observable (> 1 GeV) to unobservable energy (\sim MeV) is the common problem when we calculate ζ directly from $J_p(E)$. Guided by Indriolo et al. and Padovani et al., we adapted two extreme power-law indices $\alpha = 1$ and -1 at the low energy to extrapolate the proton spectrum from the break energy, which we set at 0.2 GeV. The former has a clear turnover, as indicated by the spacecraft measurements and the solar modulation models.^{63,66} The latter contains a weak break but no turnover as is proposed by Indriolo et al. and others,^{68,69} Both cases are shown in 10. The proton injection spectrum by Chernyakova et al. is well approximated by $J_p(E) \propto E^{-2.5}$ down to the energy 1 GeV. The gap 0.2–1 GeV was bridged by power-law spectrum with index $\alpha = -1.25$ to

imitate a smooth break. The interval of the integration $[E_1, E_2]$ was arbitrarily set to 1–10 MeV. The lower cut-off energy of the integration is often set at 1 MeV, because lower energy protons do not have sufficient range to affect on the global H_2 ionization rate. However, the ionization in this particular case can be local, and the cosmic rays with short range may well contribute to ζ_2 . The calculation therefore provides only a lower limit for ζ_2 .

Integration yields $\zeta_2 = 5.5 \times 10^{-11} \text{ s}^{-1}$ for the non-turnover case with $\alpha = -1$ and a weak break and $1.6 \times 10^{-14} \text{ s}^{-1}$ for $\alpha = 1$ with a strong turnover. The numbers are reduced to $\zeta_2 = 4.6 \times 10^{-11} \text{ s}^{-1}$ and $\zeta_2 = 3.3 \times 10^{-15} \text{ s}^{-1}$, respectively, if the break energy is raised to 0.4 GeV. In either case the cosmic-ray proton spectrum without a strong turnover is 4 orders of magnitude higher than is observed in the cloud in front of GCIRS 3. This means that, if as many relativistic protons are generated as the HESS TeV γ -ray source implies, they must be strongly damped at low energy. The requirement for damping is even stronger if the actual cut-off energy is lower than 1 MeV.

A second possible explanation for the large discrepancy is that the observed column density of H_3^+ might have led to a significant underestimate of ζ_2 . We have assumed that the abundance of H_3^+ linearly increases with ζ_2 , because the reaction of H_2^+ and H_2 is rapid enough to justify neglecting other competing processes. At high ζ_2 ($> 10^{-15} \text{ s}^{-1}$), however, destructive recombination of H_2^+ with an electron becomes non-negligible, since electrons are more populous because of the high ζ_2 .^{70,71} It seems unlikely that this can completely account for the discrepancy, however.

Finally, another factor that may need to be taken into account is the time-dependent formation rate of H_2 , which would require $\sim 10^7$ yrs to reach an equilibrium, if the formation starts from pure atomic gas.⁷¹ The dynamical timescale of the Galactic center is short (the orbital period around the $4 \times 10^6 M_\odot$ black hole in Sgr A* is 10,000 yrs at 1 pc).⁷² If the formation or destruction of H_2 is triggered by the changes of the external conditions of the cloud, the molecular hydrogen in the cloud in front of GCIRS 3 may not have enough time to reach steady state abundances balancing formation and destruction. At the beginning of the process, the abundance of H_3^+ is less dependent on ζ_2 , but

more on the H_2 abundance. ζ_2 calculated on the basis of the linear dependency on $N(H_3^+)$ may not correctly represent the actual cosmic ray ionization rate.

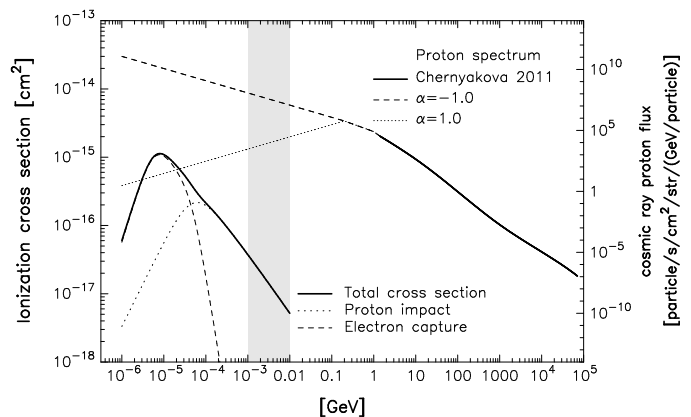


Figure 10: Proton energy distribution and ionization cross section of H_2 at 1 keV to 100 TeV. The spectrum is obtained from Chernyakova et al.⁶⁰ at $E > 1$ GeV, and is extrapolated in two ways from 0.2 GeV to 1 MeV, using $J_p(E) \propto E^{-1}$ and $J_p(E) \propto E$. The spectrum from 1 GeV to 0.2 GeV is bridged by $J_p(E) \propto E^{-1.25}$ to imitate a smooth break. See text for details. The ionization cross section is reproduced from Rudd et al.² and Padovani et al..³

X-ray ionization

Similar to the case of cosmic ray ionization, the X-ray ionization rate is the integral over energy of the product of the X-ray spectrum $F(E)$, and the ionization cross section $\sigma_x(E)$. In the X-ray regime ($0.1 \text{ keV} < E < 100 \text{ keV}$), two ionization processes must be taken into account: photo-ionization in which the X-ray photon is absorbed, and Compton scattering in which the photon is scattered at lower energy. In either case, the electron liberated by the ionization is energetic enough to lead to further ionization events on H_2 . These secondary ionizations are far more numerous than the first ionization by the X-ray photon. The photo-ionization cross section of H_2 by X-ray σ_{xp} is taken from Yan et al.⁷³ and Yan et al.,⁷⁴ and scaled by η_{xp} according to Wilms et al.⁵⁷ to take into account the contribution of the electrons produced by the photo-ionization of heavy elements. The Compton scattering cross section σ_{xc} is taken from

Hubbell et al.,⁷⁵ and scaled by η_{xc} to include the electrons from the compton scattering on helium. The photo-ionization and compton scattering cross sections are reproduced in 11. The number of secondary ionizations that follow the single primary ionization has been calculated by Dalgarno et al.⁷⁶ as a mean energy per an ion pair W , where the total number of ionization events per primary ionization N_{ion} is given by $N_{\text{ion}} = E_e/W$, with E_e being the energy of the initial (secondary) electron. Following Meijerink and Spaans,⁷⁷ we use $W(1 \text{ keV}) = 36 \text{ eV}$ over the entire energy range, as W asymptotically approaches this value for photons with $E > 1 \text{ keV}$.⁷⁶ The total X-ray ionization rate is then given by

$$\zeta_2 = \int (\sigma_{xp}\eta_{xp} + \sigma_{xc}\eta_{xc}) \frac{E}{W(1\text{keV})} F(E) dE.$$

Two possible sources of X-ray photons are present in the central few parsecs of the Galaxy: X-ray point sources in the Central Cavity and diffuse X-ray emission. At least five X-ray point sources are known within 10 arcseconds of Sgr A*,³¹ including Sgr A* and GCIRS 13, a compact star cluster that is thought to contain an intermediate-mass black hole inside.⁷⁸ All are of more or less similar brightness (10^{32} – $10^{33} \text{ erg s}^{-1}$ at 2–10 keV) with Sgr A* slightly brighter than the others.

Here we calculate the ionization rate caused by X-ray irradiation from Sgr A* as an example. The actual ζ_2 would be a few times larger if the contribution of other point sources are included. The observed X-ray luminosity of Sgr A* at 2–10 keV is $2.4 \times 10^{33} \text{ erg s}^{-1}$.³¹ In order to extrapolate the spectral range to cover 0.1 keV to 100 keV, we create a spectrum using the Raymond-Smith plasma model⁷⁹ provided in AtomDB package⁸⁰ with the plasma temperature $kT = 1.9 \text{ keV}$ as suggested by Baganoff et al.³¹ and normalized to match the above observed luminosity. The complete spectrum is shown in 11. The flux of X-ray photons that the cloud at GCIRS 3 receives is $F(E) = L_*(E)/4\pi r^2$, where r is the distance from Sgr A* to the cloud, assuming the X-ray emission is isotropic and that there is no attenuation. The resultant ζ_2 is highly dependent on the distance to the X-ray source; using the minimum linear dis-

tance between GCIRS 3 and Sgr A* projected on the sky ($\approx 0.2 \text{ pc}$), ζ_2 is $5.8 \times 10^{-13} \text{ s}^{-1}$ including the secondary ionizations, considerably larger than the value derived from the observed H_3^+ lines.

The second possible ionizing source is the local diffuse X-ray emission that extends ≈ 10 arcseconds of Sgr A*.³¹ According to Rockefeller et al.⁸¹ the emission is likely the sum of the X-ray emission from the stellar winds produced by the evolved massive stars in the Central Cluster. Its X-ray luminosity is $7.6 \times 10^{31} \text{ erg s}^{-1} \text{ arcsec}^{-2}$ (2–10 keV).³¹ The plasma temperature that best fits the observed spectrum is $kT = 1.3 \text{ keV}$. Note that “the local diffuse X-ray emission” is compact, and local to 10 arcseconds of Sgr A*. It is distinguished from the large-scale diffuse emission known as Galactic Ridge emission,⁸² and from the Sgr A halo emission, or from non-thermal emission from the supernova remnant Sgr A East, which are not included in the above value.

To estimate the ionization rate from the diffuse X-ray emission we assume a spherical X-ray emitting zone, centered on Sgr A*, of radius 1 pc, somewhat less than the inner radius of the Circumnuclear Disk, and locate the absorbing gas in front of GCIRS 3 on the surface of this sphere. The X-ray luminosity per unit volume is modeled by Rockefeller et al.⁸¹ as a function of the distance from Sgr A*. We integrate the luminosity per unit volume to determine the total luminosity generated within the sphere. Only the outward X-ray flux was taken into account. The calculation yields $\zeta_2 = 4.8 \times 10^{-13} \text{ s}^{-1}$ including the secondary ionizations, again considerably larger than the value derived from the observed H_3^+ lines. We note that it is highly dependent on the radius of the emitting sphere (e.g., if the cloud is closer to the center (0.2 pc), ζ_2 is increased to $5.5 \times 10^{-12} \text{ s}^{-1}$).

Prospects and Status

With sufficient numbers of suitable background sources such as GCIRS 1W and GCIRS 3 in the central few parsecs of the Galaxy and with a sufficiently extensive distribution of molecular gas within the Central Cavity, one should be able to use spectroscopy of H_3^+ to detect the footprints of the ionization sources and to discriminate be-

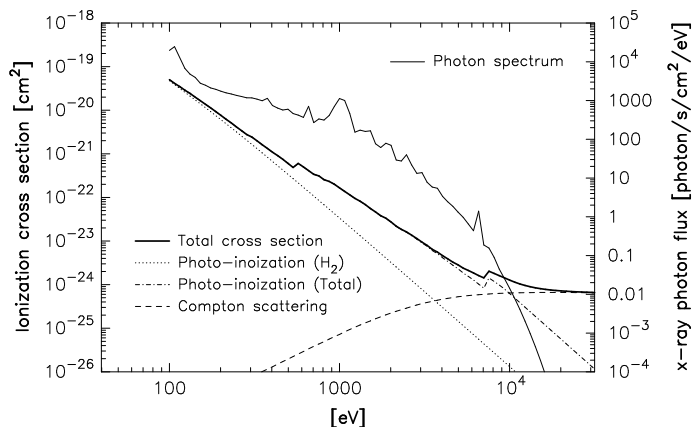


Figure 11: Calculated photon distribution of the diffuse local X-ray emission at a distance of 1 pc from Sgr A*, and the ionization cross section of H_2 , from 100 eV to 10 keV. The spectrum was calculated from the Raymond-Smith plasma model⁷⁹ provided in AtomDB⁸⁰ with the plasma temperature $kT = 1.9$ keV, and scaled so that the luminosity matches to that of Baganoff et al.³¹ modeled by Rockefeller et al..⁸¹ The photo-ionization cross is taken from Yan et al.⁷³ and Yan et al.,⁷⁴ and Compton scattering cross section is taken from Hubbell et al..⁷⁵

tween the various possibilities for ionization that have been put forth in the previous section. If X-rays are the main source of the ionization, ζ_2 should be enhanced close to the individual X-ray sources such as Sgr A* and the powerful wind source GCIRS 13. If cosmic rays (protons) are the main ionization source, ζ_2 would be enhanced at the inner wall of the Circumnuclear Disk, or on the compact clumps, where the relativistic protons encounter cold nuclei. Inside the Central Cavity, ζ_2 would gradually decrease with the distance from Sgr A*, as the protons lose energy as they propagate outward. High spatial sampling of ζ_2 is the key to address the primary ionization mechanism, and the possible in situ acceleration of cosmic rays by the black hole.

The Central Cluster contains hundreds of massive and luminous stars whose spectra are simple enough to allow quantitative spectroscopy of the H_3^+ lines from $J = 1, 2,$ and 3 levels that are needed to measure ζ_2 . The performances of current telescope and instruments limit the targets to a handful of stars brighter than $L < 7.5$ mag (or $F_\lambda > 10^{-13} \text{ W m}^{-2} \mu\text{m}^{-1}$) (labeled in 6). A pilot

survey of H_3^+ toward these stars has been carried out at the Subaru Telescope on Mauna Kea with the spectrograph IRCS, and instrument that is efficient in surveying multiple lines. All sources so far studied show significant H_3^+ absorption from $J=1$ and 3 levels (12). We intend to obtain improved spectra using CRIRES/VLT and to use it to search for the tracer of warm, dense clouds, the $R(2,2)^l$ line.

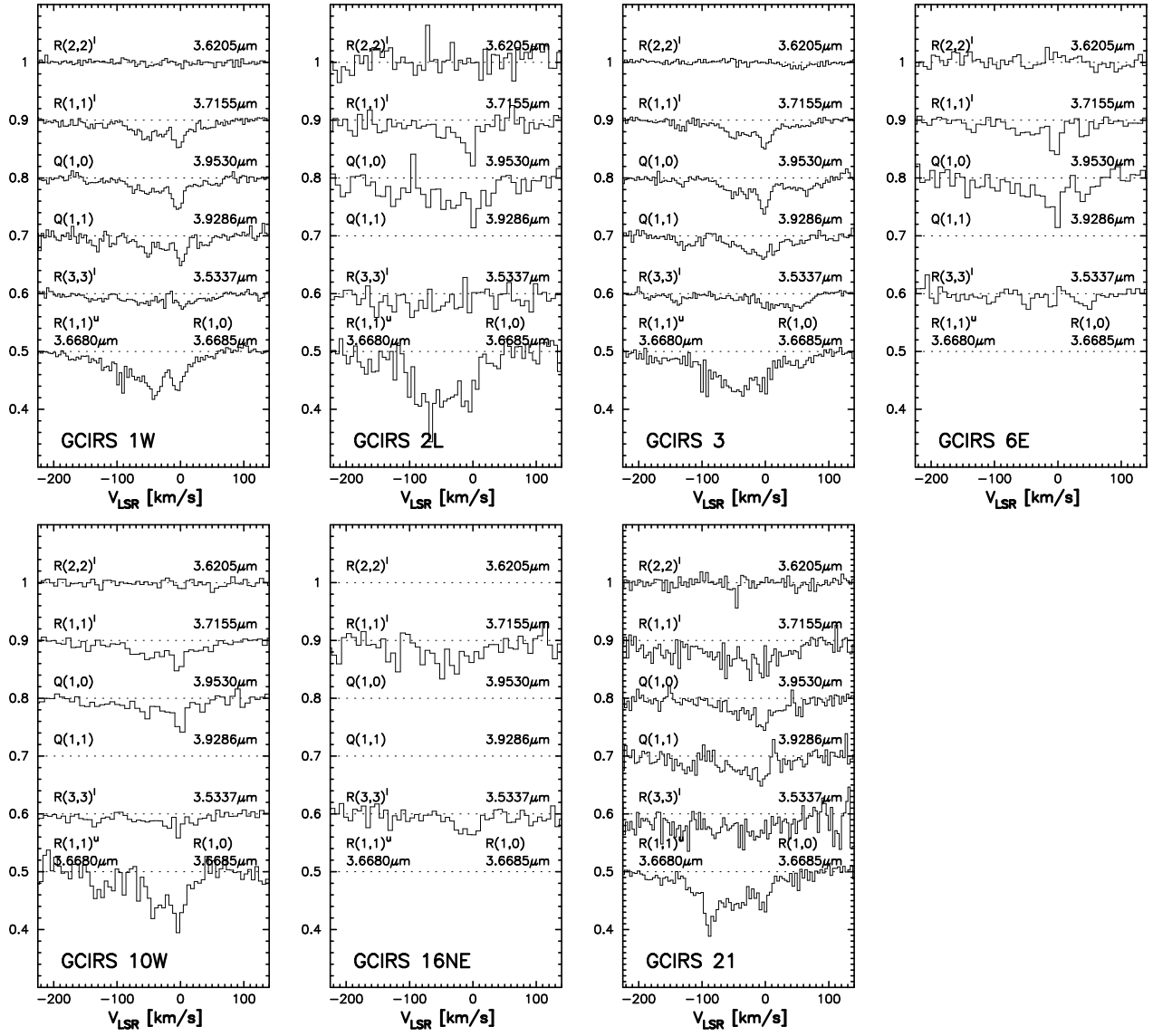


Figure 12: H_3^+ spectra toward the stars in the Central Cluster obtained in the pilot survey carried out with IRCS at the Subaru Telescope.

Acknowledgement The authors thank the VLT and the Subaru Telescope for their valuable assistance in obtaining the data. We thank María ontero-Castaño for providing HCN $J=4-3$ map in the machine-readable form. We thank Masha Chernyakova for the ascertainment of the conversion of her proton energy spectrum to the proton number count spectrum. We thank Andrii Neronov for the explanation of his proton energy spectrum. The authors are grateful to Takeshi Oka, not only for careful reading of an early draft, but also for his continuous inspiration. M.G. is supported by DFG grant GO 1927/3-1. T.R.G. is supported by the Gemini Observatory, which is operated by the Association of Universities for Research in Astronomy, Inc., on behalf of the international Gemini partnership of Argentina, Australia, Brazil, Canada, Chile, and the United States of America.

References

- (1) Herzberg, G. Dissociation Energy and Ionization Potential of Molecular Hydrogen. *Phys. Rev. Lett.* **1969**, 23, 1081–1083.
- (2) Rudd, M. E.; Goffe, T. V.; Dubois, R. D.; Toburen, L. H.; Ratcliffe, C. A. Cross Sections for Ionization of Gases by 5 - 4000 keV Protons and for Electron Capture by 5 - 150 keV Protons. *Phys. Rev. A: General Physics* **1983**, 28, 3244–3257.
- (3) Padovani, M.; Galli, D.; Glassgold, A. E. Cosmic-Ray Ionization of Molecular Clouds. *Astron. Astrophys.* **2009**, 501, 619–631.
- (4) Spitzer, L.; Tomasko, M. G. Heating of H I Regions by Energetic Particles. *Astrophys. J.* **1968**, 152, 971–986.
- (5) Black, J. H.; Dalgarno, A. Models of Interstellar Clouds. I - The Zeta Ophiuchi Cloud. *Astrophys. J., Suppl. Ser.* **1977**, 34, 405–423.
- (6) van Dishoeck, E. F.; Black, J. H. Comprehensive Models of Diffuse Interstellar Clouds - Physical Conditions and Molecular Abundances. *Astrophys. J., Suppl. Ser.* **1986**, 62, 109–145.
- (7) van der Tak, F. F. S.; van Dishoeck, E. F. Limits on the Cosmic-Ray Ionization Rate toward Massive Young Stars. *Astron. Astrophys.* **2000**, 358, L79–L82.
- (8) Geballe, T. R.; Oka, T. Detection of H_3^+ in Interstellar Space. *Nature* **1996**, 384, 334–335.
- (9) McCall, B. J.; Hinkle, K. H.; Geballe, T. R.; Moriarty-Schieven, G. H.; Evans, N. J.; Kawaguchi, K.; Takano, S.; Smith, V. V.; Oka, T. Observations of H_3^+ in the Diffuse Interstellar Medium. *Astrophys. J.* **2002**, 567, 391–406.
- (10) Indriolo, N.; Geballe, T. R.; Oka, T.; McCall, B. J. H_3^+ in Diffuse Interstellar Clouds: A Tracer for the Cosmic-Ray Ionization Rate. *Astrophys. J.* **2007**, 671, 1736–1747.
- (11) Indriolo, N.; McCall, B. J. Investigating the Cosmic-Ray Ionization Rate in the Galactic Diffuse Interstellar Medium through Observations of H_3^+ . *Astrophys. J.* **2012**, 745, 91.
- (12) Indriolo, N.; Fields, B. D.; McCall, B. J. The Implications of a High Cosmic-Ray Ionization Rate in Diffuse Interstellar Clouds. *Astrophys. J.* **2009**, 694, 257–267.
- (13) Indriolo, N.; Blake, G. A.; Goto, M.; Usuda, T.; Oka, T.; Geballe, T. R.; Fields, B. D.; McCall, B. J. Investigating the Cosmic-Ray Ionization Rate Near the Supernova Remnant IC 443 through H_3^+ Observations. *Astrophys. J.* **2010**, 724, 1357–1365.
- (14) Yusef-Zadeh, F.; Munro, M.; Wardle, M.; Lis, D. C. The Origin of Diffuse X-Ray and γ -Ray Emission from the Galactic Center Region: Cosmic-Ray Particles. *Astrophys. J.* **2007**, 656, 847–869.
- (15) Tatischeff, V.; Decourchelle, A.; Maurin, G. Nonthermal X-Rays from Low-Energy Cosmic Rays: Application to the 6.4 keV Line Emission from the Arches Cluster Region. *Astron. Astrophys.* **2012**, 546, 88.
- (16) Becker, J. K.; Black, J. H.; Safarzadeh, M.; Schuppan, F. Tracing the Sources of Cosmic Rays with Molecular Ions. *Astrophys. J., Lett.* **2011**, 739, L43.

- (17) Black, J. H. H_3^+ at the Interface between Astrochemistry and Astroparticle Physics. *Philos. Trans. R. Soc., A* **2012**, *370*, 5130–5141.
- (18) Goto, M.; Usuda, T.; Nagata, T.; Geballe, T. R.; McCall, B. J.; Indriolo, N.; Suto, H.; Henning, T.; Morong, C. P.; Oka, T. Absorption Line Survey of H_3^+ toward the Galactic Center Sources. II. Eight Infrared Sources within 30 pc of the Galactic Center. *Astrophys. J.* **2008**, *688*, 306–319.
- (19) Crocker, R. M.; Jones, D. I.; Aharonian, F.; Law, C. J.; Melia, F.; Oka, T.; Ott, J. Wild at Heart: the Particle Astrophysics of the Galactic Centre. *Mon. Not. R. Astron. Soc.* **2011**, *413*, 763–788.
- (20) Tammann, G. A.; Loeffler, W.; Schroeder, A. The Galactic Supernova Rate. *Astrophys. J., Suppl. Ser.* **1994**, *92*, 487–493.
- (21) van den Bergh, S.; Tammann, G. A. Galactic and Extragalactic Supernova Rates. *Annu. Rev. Astron. Astrophys.* **1991**, *29*, 363–407.
- (22) Morris, M.; Serabyn, E. The Galactic Center Environment. *Annu. Rev. Astron. Astrophys.* **1996**, *34*, 645–701.
- (23) Goto, M.; McCall, B. J.; Geballe, T. R.; Usuda, T.; Kobayashi, N.; Terada, H.; Oka, T. Absorption Line Survey of H_3^+ toward the Galactic Center Sources I. GCS 3-2 and GC IRS3. *Publ. Astron. Soc. Jpn.* **2002**, *54*, 951–961.
- (24) Oka, T.; Geballe, T. R.; Goto, M.; Usuda, T.; McCall, B. J. Hot and Diffuse Clouds near the Galactic Center Probed by Metastable H_3^+ . *Astrophys. J.* **2005**, *632*, 882–893.
- (25) Gillessen, S.; Eisenhauer, F.; Trippe, S.; Alexander, T.; Genzel, R.; Martins, F.; Ott, T. Monitoring Stellar Orbits Around the Massive Black Hole in the Galactic Center. *Astrophys. J.* **2009**, *692*, 1075–1109.
- (26) Krabbe, A.; Genzel, R.; Eckart, A.; Najarro, F.; Lutz, D.; Cameron, M.; Kroker, H.; Tacconi-Garman, L. E.; Thatte, N.; Weitzel, L.; et al., The Nuclear Cluster of the Milky Way: Star Formation and Velocity Dispersion in the Central 0.5 Parsec. *Astrophys. J., Lett.* **1995**, *447*, L95–L99.
- (27) Christopher, M. H.; Scoville, N. Z.; Stolovy, S. R.; Yun, M. S. HCN and HCO^+ Observations of the Galactic Circumnuclear Disk. *Astrophys. J.* **2005**, *622*, 346–365.
- (28) Montero-Castaño, M.; Herrnstein, R. M.; Ho, P. T. P. Gas Infall Toward Sgr A* from the Clumpy Circumnuclear Disk. *Astrophys. J.* **2009**, *695*, 1477–1494.
- (29) Güsten, R. Atomic and Molecular Gas in the Circumnuclear Disk. *AIP Conf. Proc.* **1987**, *155*, 19.
- (30) Requena-Torres, M. A.; Güsten, R.; Weiß, A.; Harris, A. I.; Martín-Pintado, J.; Stutzki, J.; Klein, B.; Heyminck, S.; Risacher, C. GREAT Confirms Transient Nature of the Circum-nuclear Disk. *Astron. Astrophys.* **2012**, *542*, L21.
- (31) Baganoff, F. K.; Maeda, Y.; Morris, M.; Bautz, M. W.; Brandt, W. N.; Cui, W.; Doty, J. P.; Feigelson, E. D.; Garmire, G. P.; Pravdo, S. H.; et al., Chandra X-Ray Spectroscopic Imaging of Sagittarius A* and the Central Parsec of the Galaxy. *Astrophys. J.* **2003**, *591*, 891–915.
- (32) Becklin, E. E.; Neugebauer, G. Infrared Observations of the Galactic Center. *Astrophys. J.* **1968**, *151*, 145–161.
- (33) Viehmann, T.; Eckart, A.; Schödel, R.; Moutakka, J.; Straubmeier, C.; Pott, J.-U. L- and M-Band Imaging Observations of the Galactic Center Region. *Astron. Astrophys.* **2005**, *433*, 117–125.
- (34) Paumard, T.; Genzel, R.; Martins, F.; Nayakshin, S.; Beloborodov, A. M.; Levin, Y.; Trippe, S.; Eisenhauer, F.; Ott, T.; Gillessen, S.; et al., The Two Young Star Disks in the Central Parsec of the Galaxy: Properties, Dynamics, and Formation. *Astrophys. J.* **2006**, *643*, 1011–1035.

- (35) Najarro, F.; Krabbe, A.; Genzel, R.; Lutz, D.; Kudritzki, R. P.; Hillier, D. J. Quantitative Spectroscopy of the He I Cluster in the Galactic Center. *Astron. Astrophys.* **1997**, *325*, 700–708.
- (36) Martins, F.; Genzel, R.; Hillier, D. J.; Eisenhauer, F.; Paumard, T.; Gillessen, S.; Ott, T.; Trippe, S. Stellar and Wind Properties of Massive Stars in the Central Parsec of the Galaxy. *Astron. Astrophys.* **2007**, *468*, 233–254.
- (37) Zhao, J.-H.; Morris, M. R.; Goss, W. M.; An, T. Dynamics of Ionized Gas at the Galactic Center: Very Large Array Observations of the Three-Dimensional Velocity Field and Location of the Ionized Streams in Sagittarius A West. *Astrophys. J.* **2009**, *699*, 186.
- (38) Zhao, J.-H.; Blundell, R.; Moran, J. M.; Downes, D.; Schuster, K. F.; Marrone, D. P. The High-density Ionized Gas in the Central Parsec of the Galaxy. *Astrophys. J.* **2010**, *723*, 1097–1109.
- (39) Kaeufl, H.-U.; Ballester, P.; Biereichel, P.; Delabre, B.; Donaldson, R.; Dorn, R.; Fedrigo, E.; Finger, G.; Fischer, G.; Franza, F.; et al., CRIFRES: a High-Resolution Infrared Spectrograph for ESO’s VLT. *Ground-based Instrumentation for Astronomy. Edited by Alan F. M. Moorwood and Iye Masanori. Proceedings of the SPIE* **2004**, *5492*, 1218–1227.
- (40) Eisenhauer, F.; Genzel, R.; Alexander, T.; Abuter, R.; Paumard, T.; Ott, T.; Gilbert, A.; Gillessen, S.; Horrobin, M.; Trippe, S.; et al., SINFONI in the Galactic Center: Young Stars and Infrared Flares in the Central Light-Month. *Astrophys. J.* **2005**, *628*, 246–259.
- (41) Ghez, A. M.; Salim, S.; Weinberg, N. N.; Lu, J. R.; Do, T.; Dunn, J. K.; Matthews, K.; Morris, M. R.; Yelda, S.; Becklin, E. E.; et al., Measuring Distance and Properties of the Milky Way’s Central Supermassive Black Hole with Stellar Orbits. *Astrophys. J.* **2008**, *689*, 1044–1062.
- (42) Geballe, T. R.; Oka, T. Two New and Remarkable Sightlines Through the Galactic Center’s Molecular Gas. *Astrophys. J., Lett.* **2010**, *709*, L70–L73.
- (43) Zylka, R.; Mezger, P. G.; Wink, J. E. Anatomy of the Sagittarius A Complex. I - Geometry, Morphology and Dynamics of the Central 50 to 100 pc. *Astron. Astrophys.* **1990**, *234*, 133–146.
- (44) Mezger, P. G.; Duschl, W. J.; Zylka, R. The Galactic Center: a Laboratory for AGN? *The Astronomy and Astrophysics Review* **1996**, *7*, 289–388.
- (45) Neale, L.; Miller, S.; Tennyson, J. Spectroscopic Properties of the H_3^+ Molecule: A New Calculated Line List. *Astrophys. J.* **1996**, *464*, 516–520.
- (46) Oka, T.; Epp, E. The Nonthermal Rotational Distribution of H_3^+ . *Astrophys. J.* **2004**, *613*, 349–354.
- (47) Kramer, C.; Jakob, H.; Mookerjea, B.; Schneider, N.; Brüll, M.; Stutzki, J. Emission of CO, C I, and C II in W3 Main. *Astron. Astrophys.* **2004**, *424*, 887–903.
- (48) Anicich, V. G.; Huntress, W. T. A Survey of Bimolecular Ion-molecule Reactions for Use in Modeling the Chemistry of Planetary Atmospheres, Cometary Comae, and Interstellar Clouds. *Astrophys. J., Suppl. Ser.* **1986**, *62*, 553–672.
- (49) Klippenstein, S. J.; Georgievskii, Y.; McCall, B. J. Temperature Dependence of Two Key Interstellar Reactions of H_3^+ : $\text{O}(^3\text{P}) + \text{H}_3^+$ and $\text{CO} + \text{H}_3^+$. *J. Phys. Chem. A* **2010**, *114*, 278–290.
- (50) Sofia, U. J.; Lauroesch, J. T.; Meyer, D. M.; Cartledge, S. I. B. Interstellar Carbon in Translucent Sight Lines. *Astrophys. J.* **2004**, *605*, 272–277.
- (51) Lacy, J. H.; Knacke, R.; Geballe, T. R.; Tokunaga, A. T. Detection of Absorption by H_2 in Molecular Clouds: A Direct Measurement of the $\text{H}_2:\text{CO}$ Ratio. *Astrophys. J.* **1994**, *428*, L69–L72.

- (52) Sodroski, T. J.; Odegard, N.; Dwek, E.; Hauser, M. G.; Franz, B. A.; Freedman, I.; Kelsall, T.; Wall, W. F.; Berriman, G. B.; Odenwald, S. F.; et al., The Ratio of H₂ Column Density to ¹²CO Intensity in the Vicinity of the Galactic Center. *Astrophys. J.* **1995**, *452*, 262–268.
- (53) Arimoto, N.; Sofue, Y.; Tsujimoto, T. CO-to-H₂ Conversion Factor in Galaxies. *Publ. Astron. Soc. Jpn.* **1996**, *48*, 275–284.
- (54) Rolleston, W. R. J.; Smartt, S. J.; Dufton, P. L.; Ryans, R. S. I. The Galactic Metallicity Gradient. *Astron. Astrophys.* **2000**, *363*, 537–554.
- (55) Chiappini, C.; Matteucci, F.; Romano, D. Abundance Gradients and the Formation of the Milky Way. *Astrophys. J.* **2001**, *554*, 1044–1058.
- (56) Esteban, C.; García-Rojas, J.; Peimbert, M.; Peimbert, A.; Ruiz, M. T.; Rodríguez, M.; Carigi, L. Carbon and Oxygen Galactic Gradients: Observational Values from H II Region Recombination Lines. *Astrophys. J.* **2005**, *618*, L95–L98.
- (57) Wilms, J.; Allen, A.; McCray, R. On the Absorption of X-Rays in the Interstellar Medium. *Astrophys. J.* **2000**, *542*, 914–924.
- (58) Aharonian, F.; Akhperjanian, A. G.; Aye, K.-M.; Bazer-Bachi, A. R.; Beilicke, M.; Benbow, W.; Berge, D.; Berghaus, P.; Bernlöhr, K.; Bolz, O.; et al., Very High Energy Gamma Rays from the Direction of Sagittarius A*. *Astron. Astrophys.* **2004**, *425*, L13–L17.
- (59) Aharonian, F.; Neronov, A. TeV Gamma Rays From the Galactic Center Direct and Indirect Links to the Massive Black Hole in Sgr A. *Astrophys. Space Sci.* **2005**, *300*, 255–265.
- (60) Chernyakova, M.; Malyshev, D.; Aharonian, F. A.; Crocker, R. M.; Jones, D. I. The High-Energy, Arcminute-Scale Galactic Center Gamma-Ray Source. *Astrophys. J.* **2011**, *726*, 60.
- (61) Bethe, H. Handbuch der Physik: Aufbau der zusammenhängenden Materie. *Handbuch der Physik* **1933**,
- (62) Webber, W. R. A New Estimate of the Local Interstellar Energy Density and Ionization Rate of Galactic Cosmic Rays. *Astrophys. J.* **1998**, *506*, 329–334.
- (63) Webber, W. R.; Higbie, P. R. Galactic Propagation of Cosmic Ray Nuclei in a Model with an Increasing Diffusion Coefficient at Low Rigidities: A Comparison of the New Interstellar Spectra with Voyager Data in the Outer Heliosphere. *J. Geophys. Res.* **2009**, *114*, A02103.
- (64) Langner, U. W.; Potgieter, M. S. Modulation of Galactic Protons in an Asymmetrical Heliosphere. *Astrophys. J.* **2005**, *630*, 1114–1124.
- (65) Scherer, K.; Fichtner, H.; Strauss, R. D.; Ferreira, S. E. S.; Potgieter, M. S.; Fahr, H.-J. On Cosmic Ray Modulation beyond the Heliosphere: Where is the Modulation Boundary? *Astrophys. J.* **2011**, *735*, 128.
- (66) Moskalenko, I. V.; Strong, A. W.; Ormes, J. F.; Potgieter, M. S. Secondary Antiprotons and Propagation of Cosmic Rays in the Galaxy and Heliosphere. *Astrophys. J.* **2002**, *565*, 280–296.
- (67) Cravens, T. E.; Dalgarno, A. Ionization, Dissociation, and Heating Efficiencies of Cosmic Rays in a Gas of Molecular Hydrogen. *Astrophys. J.* **1978**, *219*, 750–752.
- (68) Neronov, A.; Semikoz, D. V.; Taylor, A. M. Low-Energy Break in the Spectrum of Galactic Cosmic Rays. *Phys. Rev. Lett.* **2012**, *108*, 51105.
- (69) Nath, B. B.; Gupta, N.; Biermann, P. L. Spectrum and Ionization Rate of Low-Energy Galactic Cosmic Rays. *Mon. Not. R. Astron. Soc.: Lett.* **2012**, *425*, L86–L90.
- (70) Liszt, H. S. H₃⁺ in the Diffuse Interstellar Medium. *Philos. Trans. R. Soc., A* **2006**, *364*, 3049–3062.

- (71) Liszt, H. S. Time-dependent H₂ Formation and Protonation in Diffuse Clouds. *Astron. Astrophys.* **2007**, *461*, 205–214.
- (72) Genzel, R.; Eisenhauer, F.; Gillessen, S. The Galactic Center Massive Black Hole and Nuclear Star Cluster. *Rev. Mod. Phys.* **2010**, *82*, 3121–3195.
- (73) Yan, M.; Sadeghpour, H. R.; Dalgarno, A. Photoionization Cross Sections of He and H₂. *Astrophys. J.* **1998**, *496*, 1044–1050.
- (74) Yan, M.; Sadeghpour, H. R.; Dalgarno, A. Erratum: Photoionization Cross Sections of He and H₂. *Astrophys. J.* **2001**, *559*, 1194.
- (75) Hubbell, J. H.; Veigele, W. J.; Briggs, E. A.; Brown, R. T.; Cromer, R. T.; Howerton, R. J. Atomic Form Factors, Incoherent Scattering Functions, and Photon Scattering Cross Sections. *J. Phys. Chem. Ref. Data* **1975**, *4*, 471–538.
- (76) Dalgarno, A.; Yan, M.; Liu, W. Electron Energy Deposition in a Gas Mixture of Atomic and Molecular Hydrogen and Helium. *Astrophys. J., Suppl. Ser.* **1999**, *125*, 237–256.
- (77) Meijerink, R.; Spaans, M. Diagnostics of Irradiated Gas in Galaxy Nuclei. I. A Far-Ultraviolet and X-Ray Dominated Region Code. *Astron. Astrophys.* **2005**, *436*, 397–409.
- (78) Maillard, J. P.; Paumard, T.; Stolovy, S. R.; Rigaut, F. The Nature of the Galactic Center Source IRS 13 Revealed by High Spatial Resolution in the Infrared. *Astron. Astrophys.* **2004**, *423*, 155–167.
- (79) Raymond, J. C.; Smith, B. W. Soft X-ray Spectrum of a Hot Plasma. *Astrophys. J., Suppl. Ser.* **1977**, *35*, 419–439.
- (80) Foster, A. R.; Ji, L.; Smith, R. K.; Brickhouse, N. S. Updated Atomic Data and Calculations for X-Ray Spectroscopy. *Astrophys. J.* **2012**, *756*, 128.
- (81) Rockefeller, G.; Fryer, C. L.; Melia, F.; Warren, M. S. Diffuse X-Rays from the Inner 3 Parsecs of the Galaxy. *Astrophys. J.* **2004**, *604*, 662–670.
- (82) Koyama, K.; Maeda, Y.; Sonobe, T.; Takeshima, T.; Tanaka, Y.; Yamauchi, S. ASCA View of Our Galactic Center: Remains of Past Activities in X-Rays? *Publ. Astron. Soc. Jpn.* **1996**, *48*, 249–255.